Vol. 38 No. 3 Journal of the Communications Research Laboratory November 1991
Printed in Tokyo, Japan pp. 417 – 433

III. VLBI SYSTEM

III. 1 VLBI ANTENNAS OF THE COMMUNICATIONS RESEARCH LABORATORY

By
Hiroshi TAKABA

(Received on March 18, 1991)

ABSTRACT

The Communications Research Laboratory has four antennas dedicated to VLBI observations, the diameters are 3 m, 10 m, 26 m, and 34 m. The two largest antennas, 26 m and 34 m, are used mainly for international VLBI experiments: geodesy, earth rotation study, and radio astronomy. The 3-m antenna and the 10-m antenna are used for domestic geodesy VLBI experiments.

The 26-m antenna of the Kashima Space Research Center has S/X band receivers and has been used for international VLBI experiments since 1984. The 3-m antenna, which is the world smallest VLBI station, was developed for mobile experiments. The 10-m antenna at Marcus Island and the 34-m antenna at Kashima were completed in 1988. They are key stations in the Western Pacific VLBI network for monitoring tectonic plate motion around Japan. The surface accuracy of the 34-m antenna is 0.17 mm (rms). This enables it to be used at millimeter wavelengths. Ten low-noise radio astronomy frequency-band receivers from 300 MHz to 43 GHz are installed on the antenna.

This paper describes the performance of CRL's VLBI antennas and gives details of the new 34-m antenna system including a new antenna pointing calibration method for medium-sized antennas.

1. Introduction

1.1 26-m Antenna

The Communications Research Laboratory (CRL) has been conducting international VLBI experiments since 1984 using the 26-m antenna (Fig. 1) at the Kashima space Research Center (KSRC) to investigate global plate motions[1], earth rotation studies[2], radio astrometric research[3], and for international time services[4]. This antenna was constructed in 1968 in order to conduct satellite communications experiments at 4 GHz. The system was reorganized in 1983 for VLBI observations in the 2- and 8-GHz bands.

1.2 3-m Antenna

CRL has developed VLBI techniques, which make the K-3 VLBI backend system fully compatible with the Mark-III VLBI backend system[5]. The K-4 VLBI backend system[6] is a very compact system suitable for mobile VLBI experiments. The 3-m antenna (Fig. 1) has been specially developed for mobile

Fig. 1 26-m antenna (left) of the Kashima Space Research Center and 3-m antenna (a mobile station).

VLBI experiments and it is the world's smallest VLBI station. Since 1988, several sessions of geodetic VLBI experiments have been completed by transporting the 3-m antenna to Koganei, Wakkanai, Okinawa, and Minamidaito-Island[7].

1.3 10-m Antenna and 34-m Antenna

The 10-m antenna (Fig. 2) at Marcus Island and the 34-m antenna (Fig. 3) at KSRC were constructed in 1988. These two antennas are key stations in the Western Pacific VLBI network[8] for monitoring tectonic plate motion around Japan. The first Western Pacific VLBI experiment was held in July 1989 and the precise position of Marcus Island was determined[9]. The movement of Marcus Island was measured by comparing the results with those of the second VLBI session held in June 1990[10].

Both antennas were made in the USA and it was the first attempt to import such large antennas from the USA. The 10-m antenna was supplied by Scientific Atlant Company and the 34-m antenna by TIW Systems Inc. They were imported by Rikei Japan and construction was by Nippon Electric Systems Inc.

Several new techniques are used with the 10-m and 34-m antennas. The 10-m antenna is equipped with a frequency selective subreflector (FSS) which uses both the prime-focus for S band and the cassegrain-focus for X band. The 34-m antenna uses a computer controlled feed system to allow reception of a wide frequency band from 300 MHz to 43 GHz using either the prime-focus or the cassegrain-focus.

Due to the age of the 26-m antenna, international VLBI experiments on geodesy and earth rotation have been using the 34-m antenna since March 1990. More than 30 sessions of VLBI experiments had been conducted in 1990 using the 34-m antenna.

The surface accuracy of the 34-m antenna is sufficient for millimeter wavelengths. Pointing accuracy of 7" (rms) were obtained when observing H_2O maser sources at 22 GHz.

Besides geodetic VLBI experiments, the 34-m antenna has been used for new radio astronomical

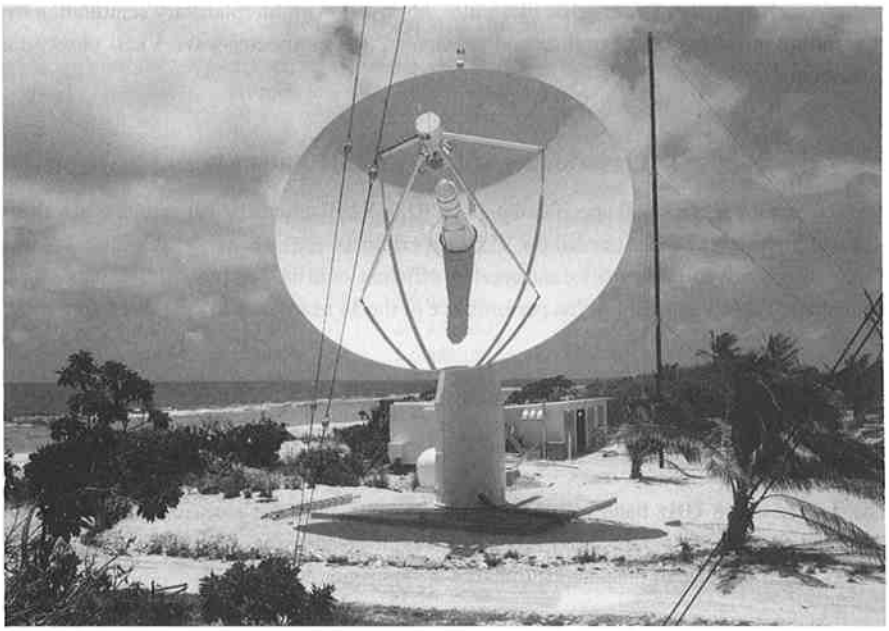

Fig. 2 10-m antenna at Marcus Island. VLBI terminals are in the building behind the antenna.

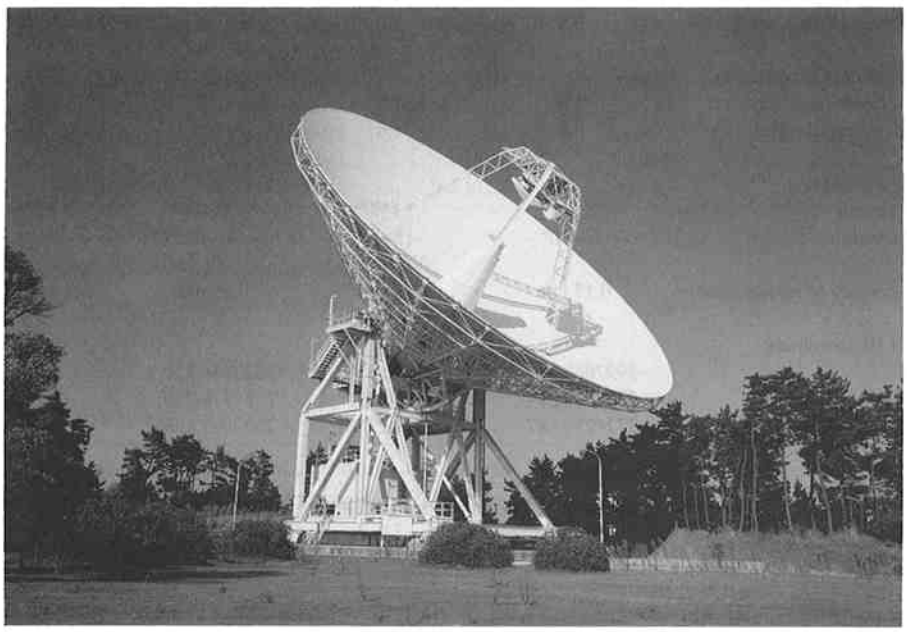

Fig. 3 34-m antenna of the Kashima Space Research Center.

observations such as study of interstellar molecules, observation of interplanetary scintillation by solar wind[11], timing measurement of millisecond pulsars[12], and millimeter-wave VLBI observation for radio astronomy[13].

2. Performance of CRL's VLBI Antennas

Table 1 lists the mechanical specifications of CRL's VLBI antennas. All antennas are altazimuth mounted and high slew speed is needed for VLBI experiments.

Table 2 lists receivers performance and aperture efficiencies in the 2 GHz and 8 GHz bands for CRL's VLBI antennas. Table 3 and Table 4 list performance of the 34 m antenna in the other frequency bands.

3. Characteristics of CRL's VLBI Antennas

3.1 26-m Antenna

The 2 GHz and 8 GHz band receivers of the 26-m antenna use electrically cooled parametric amplifiers and are at the cassegrain-focus. A beam-waveguide feed system is used. This antenna is suitable for geodesy VLBI because of the antenna mouting is very rigid.

Table 1 Mechanical specifications

Antenna diameter	34 m	26 m	10 m	3 m
Maximum speed				
Azimuth (deg./sec.)	1.0	1.0	11	10
Elevation (deg./sec.)	0.8	1.0	5	10
Maximum acceleration				
Azimuth (deg./sec. ^{2})	1.0	1.0	7.5	4.5
Elevation (deg./sec. ^{2})	0.8	1.0	2.5	3.6
Drive range				
Azimuth	±359°	±359°	±360°	±270°
Elevation	6°–90°	–1°–95°	–2°–182°	–2°–182°
Accuracy of surface (rms)	0.17 mm	0.8 mm	0.86 mm	not measured
VLBI coordinate				
X	–3997647.330	–3997890.355	–5227444.950	
Y	3276690.014	3276580.525	2551378.730	
Z	3724279.387	3724118.788	2607605.398	

Table 2 Receivers and efficiencies

Antenna	34 m	26 m	10 m	3 m
2 GHz (Tsys, η)	71 K, 68%	120 K, 52%	100 K, 55%	
8 GHz (Tsys, η)	52 K, 68%	130 K, 55%	170 K, 50%	120 K, 37%

Table 3 Beam size and efficiency

Frequency	HPBW	Efficiency η_A
300 MHz	1.8 deg	49%
600 MHz	1.0 deg*	40%*
1.5 GHz	24 arcmin.	68%
2.2 GHz	16 arcmin.	65%
5.0 GHz	7.5 arcmin.	70%
8.2 GHz	4.4 arcmin.	68%
10 GHz	3.6 arcmin.	65%
15 GHz	2.4 arcmin.	60%
22 GHz	1.6 arcmin.	57%
43 GHz	0.8 arcmin.	40 ± 10%

* Specification

Table 4 Receive band and noise temperature

Band	Frequency	Band width	Trec	Tsys
300 MHz	312–342 MHz	30 MHz	43 K	200 K
600 MHz	580–640 MHz	60 MHz	58 K	150 K*
1.5 GHz	1.35–1.75 GHz	400 MHz	10 K	38 K
2.2 GHz	2.15–2.35 GHz	200 MHz	11 K	71 K
4.8 GHz	4.6–5.1 GHz	500 MHz	29 K	55 K
8.2 GHz	7.86–8.68 GHz	820 MHz	13 K	52 K
10 GHz	10.2–10.7 GHz	500 MHz	43 K	70 K
15 GHz	14.4–15.4 GHz	1000 MHz	45 K	100 K
22 GHz	21.9–22.4 GHz	500 MHz	50–90 K	150–190 K
	23.5–24.0 GHz	500 MHz	50–90 K	160–200 K
43 GHz	42.9–43.4 GHz	500 MHz	400 K	800 K

* Specification

Tsys including the sky noise at El = 90°

3.2 3-m Antenna

An ambient temperature 8 GHz band receiver is located at the cassegrain-focus. The main dish and the mounting can be easily divided into two parts and the antenna is highly transportable.

3.3 10-m Antenna

A frequency selective subreflector (FSS) is used with the 10-m antenna (Fig. 4) to receive two bands simultaneously. This cancels the delay time caused by the earth's ionosphere. The 2 GHz band receiver

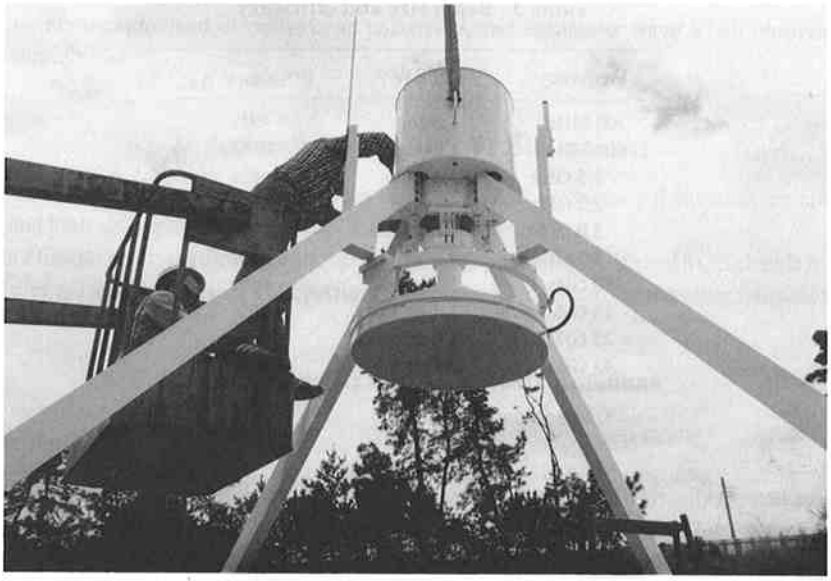

Fig. 4 Frequency Selective Subreflector (FSS) of the 10-m antenna. S band signals are not reflected by the subreflector but are collected at the prime focus. The subreflector is effective for the X band.

is at the prime-focus and the 8 GHz band receiver is at the cassegrain-focus. Both the receivers are ambient temperature types.

3.4 34-m Antenna

The surface panels of the 34-m antenna were adjusted at on elevation of 45° to a shaped parabola

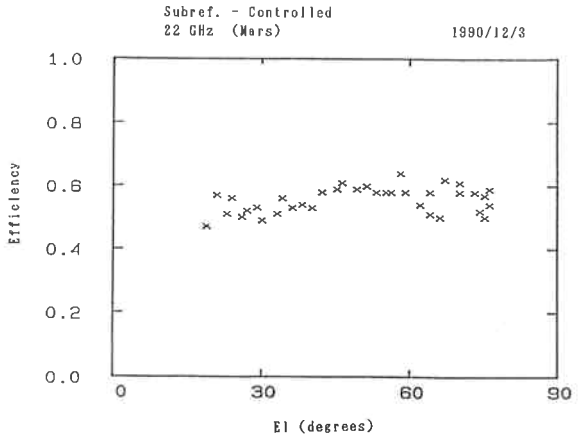

Fig. 5 Efficiency of the 34-m antenna at 22 GHz when the subreflector position is controlled as a function of the elevation.

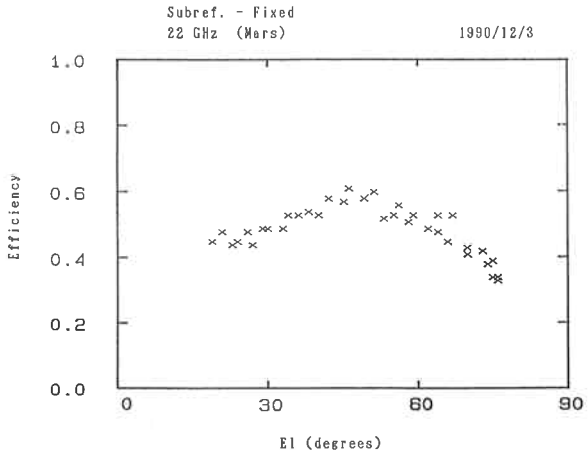

Fig. 6 Same as Fig. 4 but with the subreflector fixed at the best position of 45° elevation.

within 0.17 mm (rms). The effect of deformation by gravitation, wind pressure, temperature gradient, and solar radiation, typically reduces the accuracyr to around 0.3 mm (rms) during operation, but this is still good enough for millimeter wavelengths.

The 34-m antenna has a subreflector control mechanism to allow use of offset feed horns. Five motors and positioners control the positions of five axes with 0.01 mm accuracy. The subreflector control mechanism also serves to cancel the effect of gravitational deformation. Figure 5 shows the effect of the subreflector control as a function of elevation, nearly constant aperture efficiency was obtained from 20° to 70° at 22 GHz. Figure 6 shows the aperture efficiency with the fixed subreflector; the efficiency is reduced to a half at 70° elevation compared to 45° elevation.

The 300 MHz and 600 MHz band receivers of the 34-m antenna are ambient temperature receivers and are attached to the side of the subreflector (Fig. 7). A lateral shifter mechanism is used to move those feeds and receivers to the prime-focus at the me of observation. The other receivers from 1.5 GHz to 43 GHz bands are cooled to 15K by closed-cycle gas-helium refrigerators. The 43 GHz band receiver were developed in the Nobeyama Radio Observatory (NRO), Fuiitsu HEMT amplifiers were used.

A computer controlled feed system is needed to position such a variety of receivers. As with the lateral shifter mechanism, the trolley mechanism is used for the cassegrain-focus. Four pairs of rails are attached to the inside of the feed cone and four groups of receivers including feed horns, cryogenically cooled low noise amplifiers (LNA), and downconverters are on the rails (Fig. 8). At observation time the selected receiver is moved to the cassegrain-focus by a computer controlled motor and the others remain at the bottom. When the lateral shifter or trolley mechanism is needed, interchange of the receivers typically takes 10 minutes. However, it takes less than one minute when changing receivers which are on the same trolley such as 15 GHz/22 GHz/43 GHz band or 5/10 GHz. In this case only the subreflector's motors need to be used for receiver interchange.

Figure 9 is the schematic diagram of the 34-m antenna control system. Although several computers are used, a host computer has overall control of the system, i.e. antenna, receivers, and VLBI backend in accordance with the observation schedule.

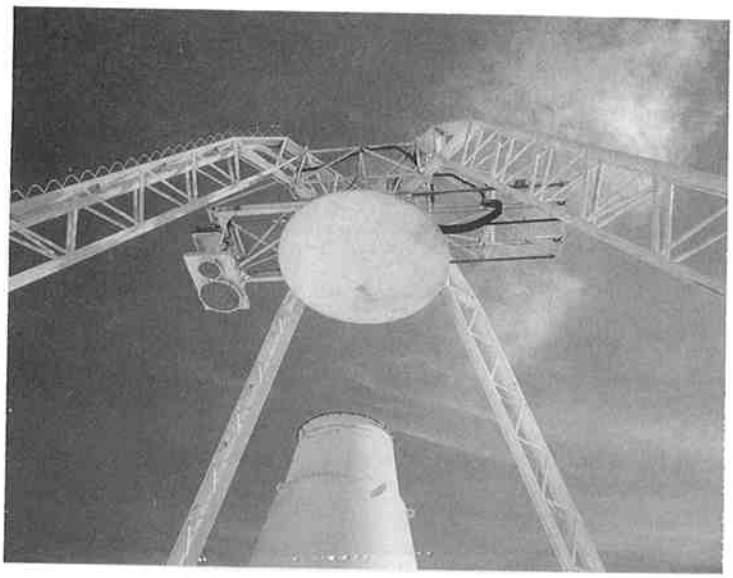

Fig. 7 Subreflector and 300 MHz/600 MHz feeds of the 34-m antenna. 300 MHz/600 MHz feeds are moved to the prime focus by a computer controlled motor at the time of observation.

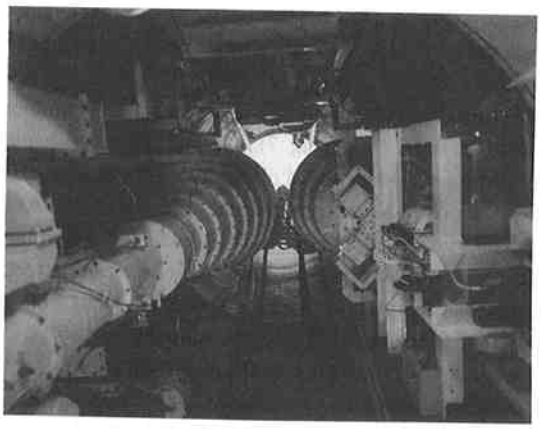

Fig. 8 Feed cone internals. Feed horns and receivers are attached to rails and move up to the cassegrain focus from the coentrol room.

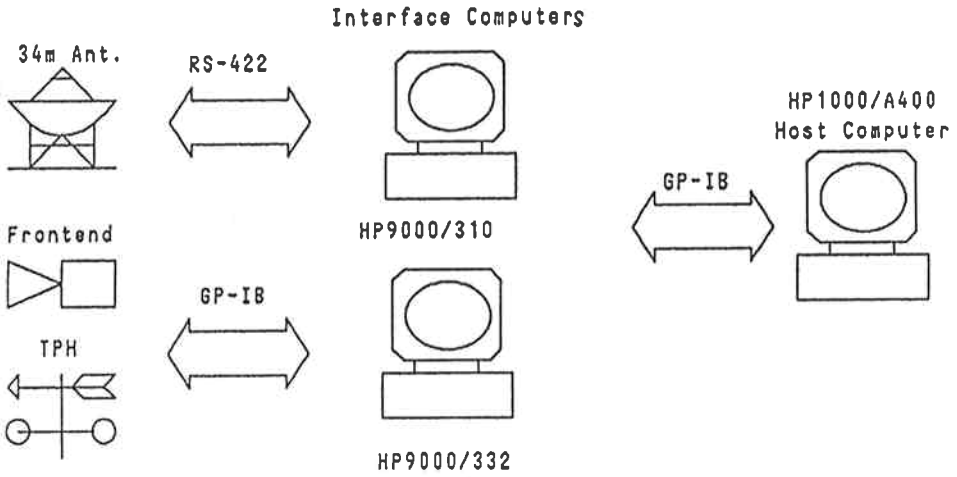

Fig. 9 Schematic diagram of the control system for the 34-m antenna.

4. A new Pointing Calibration Method

Seven pointing parameters are typically used for radio telescopes[14]. These are encoder offsets for azimuth and elevation, the collimation error between the mechanical axis and the radio beam, the inclination of the azimuth axis from the vertical direction and it's angle from the north direction, the skew angle of the elevation axis, and the first order term of gravitational deformation.

Many kinds of pointing observations have been made so far in order to measure these parameters for many antennas. For very small antennas, a small optical telescope mounted on the antenna is used to determine the pointing parameters with the exceptions of the collimation error and the gravitational effect. The telescope is used to observe bright stars at night[15]. Radio observations of the Sun and the Moon are used to determine the collimation error and the gravitational term. Strong galactic continuum sources (Cas-A, Ori-A, Virgo-A and Tau-A) are useful for medium-sized antennas such as the 10-m and the 26-m CRL antenna[16]. Strong extragalactic continuum sources (Quasars and BL Lac objects) are also used for medium-sized antennas which have very low noise receivers and precise detection systems.

The antenna beam size becomes smaller as the diameter of the antenna increases and as the observed frequency increases, thus strong radio point sources are needed to obtain very accurate pointing parameters. Consequently, strong quasars or strong maser sources are the most useful for obtaining these parameters.

The 34-m antenna is believed to be one of the best instruments for pointing observations because of the wide frequency range of the receivers. Many kinds of radio sources can be observed in different frequency ranges.

The above method were used to determine pointing parameters for the 34-m antenna in three steps: 1) observation of strong galactic continuum sources at 8 GHz, 2) observation of strong extragalactic sources at 8 GHz, and 3) observation of strong galactic H_2O maser sources at 22 GHz. An HP1000/A400 computer was used both for data acquisition and data reduction. Data were obtained for radio continuum sources using a power meter and for maser sources using a spectrum analyzer. As the central frequency

of a maser source changes due to the doppler effect of the earth[17], the velocity of the observatory relative to the source was calculated by the computer and sent to the spectrum analyzer to detect the maser emission in the central part of the local frequency sweep region.

H_2O masers at 22.235 GHz emit from circumstellar envelopes of either young stars or late-type stars and the extents of the sources are typically within 0.002°. Although the received intensities depend on the gain of the antenna, some sources are detected at more than 100 K by the 34-m antenna and were easily detected by a local sweep-type spectrum analyzer.

Figure 10 shows an example of an H_2O maser source from W49 obtained by the 34 m antenna. The

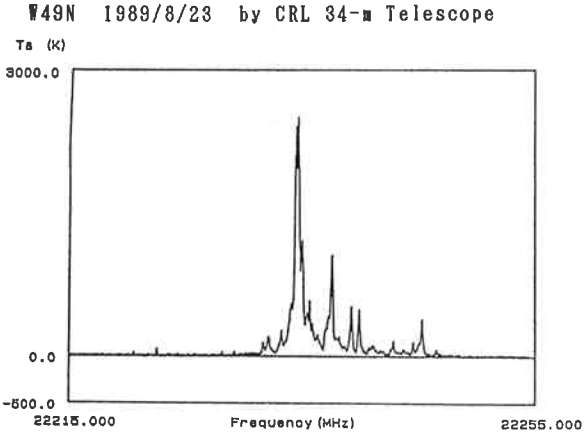

Fig. 10 H_2O maser spectrum of W49 obtained by a sweep type spectrum analyzer.

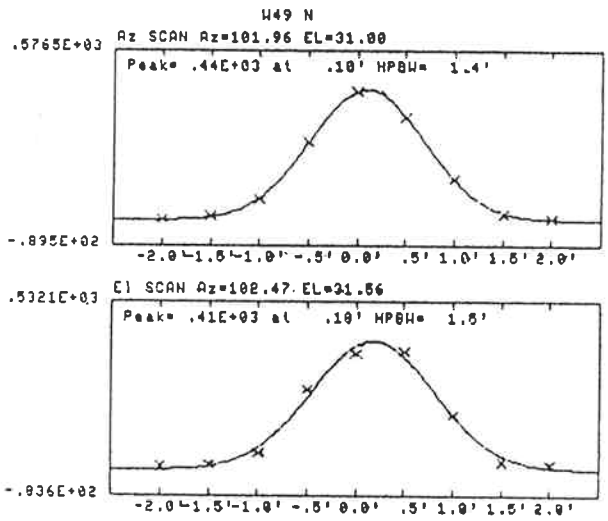

Fig. 11 An example of a cross scan at 22 GHz. Upper graph is the azimuth scan and the lower graph is the elevation scan. Crosses are the data points.

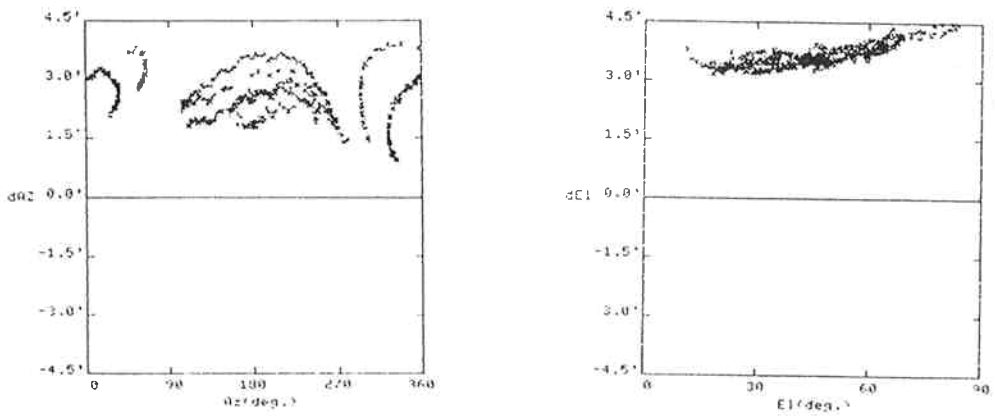

Fig. 12 Observed pointing error of the 34-m antenna with no pointing correction.

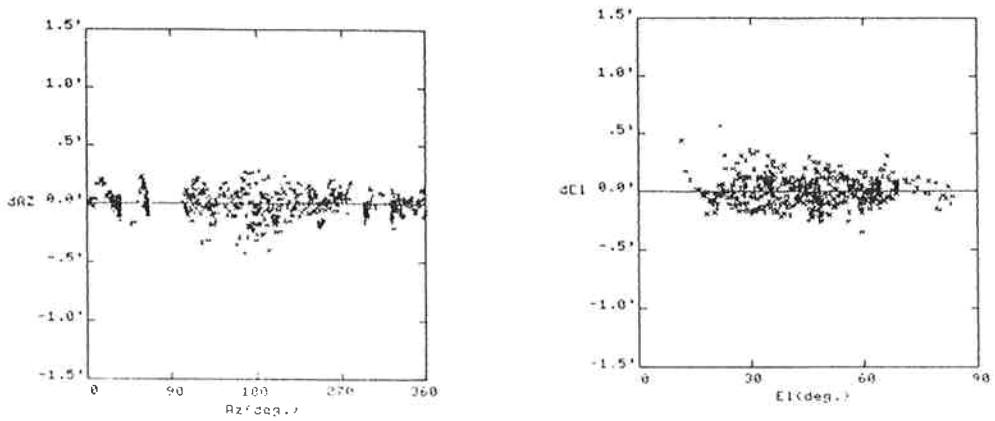

Fig. 13 Residuals of the least square fitting. 14-term pointing parameters are used.

advantage of observing maser sources compared to radio continuum sources is that the baseline of the spectra can be removed by using non-emitting channels for maser sources. Thus sky and receiver gain fluctuations that cause a serious ploblem in determining the intensities of radio sources at higher frequency can be removed.

Figure 11 shows an example of a cross scan in azimuth and in elevation axis. Data were taken from a spectrum analyzer, and after removing the baseline, the integrated intensities of the emission were calculated for each point. The pointing errors and the half power beam width were obtained by a least square gaussian fitting program. Data were stored on a computer disk and the fitting results were displayed immediately on the CRT. Figure 12 shows the observed pointing error for observations with no pointing correction. Observations were made using the pointing parameters obtained from the previous observations. Typical pointing errors were within 0.5 arc-minutes. Figure 13 shows the fitting residuals. A 14-term

pointing model was used. This included 7-term parameters, non-linear gravitational loading, and the encoder errors because systematic errors were found both in azimuth and in elevation as a function of azimuth and elevation from the residuals of the normal 7-term pointing model.

The 14-term pointing correction model equation is as follows:

$$dAz = x \cdot \sin(Az - \omega) \cdot \tan(El) + \varepsilon \cdot \tan(El) + \delta / \cos(El) + \Delta Az + A1 \cdot \sin(Az - A3) + A2 \cdot \sin(2(Az - A4)),$$

$$dEl = x \cdot \cos(Az - \omega) + G \cdot El + G1 \cdot (1 - \cos(El - 45)) + \Delta El.$$

The pointing parameters of the 34-m antenna obtained by these observations are listed in Table 5 and

Table 5

χ	=	0.0013
ω	=	139.348
ε	=	0.0041
δ	=	0.0670
G	=	0.000243
G1	=	0.03610
ΔAz	=	–0.0419
ΔEl	=	0.0481
A1	=	0.0053
A2	=	0.0101
A3	=	18.749
A4	=	8.852

Table 6

Object	R.A. (1950)	Decl. (1950)	Vlsr (km/s)	S (Jy)
W3 (OH)	02h23m17.3s	+61°38'58.2"	–48.0	1000
Ori-KL	05h32m47.0s	–05°24'23.0"	5.5	10000
VY CMa	07h20m54.6s	–25°40'12.5"	19.0	800
R Crt	10h58m06.0s	–18°03'21.0"	10.0	300
RT VIR	13h00m05.7s	+05°27'22.0"	21.5	400
W49N	19h07m49.8s	+09°01'17.0"	10.0	7000
W51	19h21m26.2s	+14°24'44.0"	55.0	4000
W75N	20h36m50.5s	+42°27'01.0"	14.0	700

the strong H_2O maser sources are listed in Table 6. A pointing accuracy of 7" (rms) is obtained.

The efficiency of the sweep type spectrum analyzer was less than 10% because it detected the signal for only a limited time during the sweep. When a 100% efficient spectrometer such as a filter bank spectrum analyzer or an acousto-optical spectrometer was used, a 10-m diameter antenna detected H_2O maser sources with the same signal to noise ratio as the 34-m antenna.

5. Examples of Observations Using the 34-m Antenna

As the 34-m antenna is equipped with a variety of low noise receivers, many kinds of radio astronomical observations are possible.

Three Solar radio maps for 2 GHz, 8 GHz and 22 GHz bands are shown in Fig. 14. It is possible for all receivers to change receiving polarization either to right hand circular polarization (RHCP) or left hand circular polarization (LHCP). It was very interesting to observe active regions on the Sun by changing the observation frequency and the polarization in order to investigate the characteristics of the temperature, electron density, and strength of magnetic fields etc.

A portable acoust-optical spectrometer (AOS, Fig. 15) which was developed in Nobeyama Radio Observatory was tested using the 34-m antenna. Figure 16 shows SiO (J = 1 – 0) maser spectra in the 43 GHz band obtained from the 34-m antenna. SiO masers are emitted from oxygen-rich late-type stars and also from some massive star forming regions. The J = 1 – 0, v = 3 transition survey conducted by Alcolea[18] *et al.* (1989) did not detect maser emission of R Aqr. Our observation was the first detection of this transition in R Agr.

The 34-m antenna is entirely computer controlled and most of the observations (VLBI, pointing calibration, continuum source mapping, and molecular spectral line survey) are done automatically in accordance with the observation schedule.

6. Conclusion

Each of CRL's four VLBI antennas has unique characteristics for its own special purpose: the small 3-m antenna is for mobile experiments; the 10-m antenna has a frequency selective subreflector for obtaining S/X band data simultaneously in order to cancel the delay time due to the earth's ionosphers; the 26-m antenna has a very stiff structure; the 34-m antenna has a computer controlled feed system.

A new pointing calibration method using the 34-m antenna is applicable to medium-sized antennas.

Using these antennas, CRL will be able to expand the application fields of VLBI. Also the new 34-m antenna has the capability of using a single dish for engineering development experiments and a wide range of scientific research.

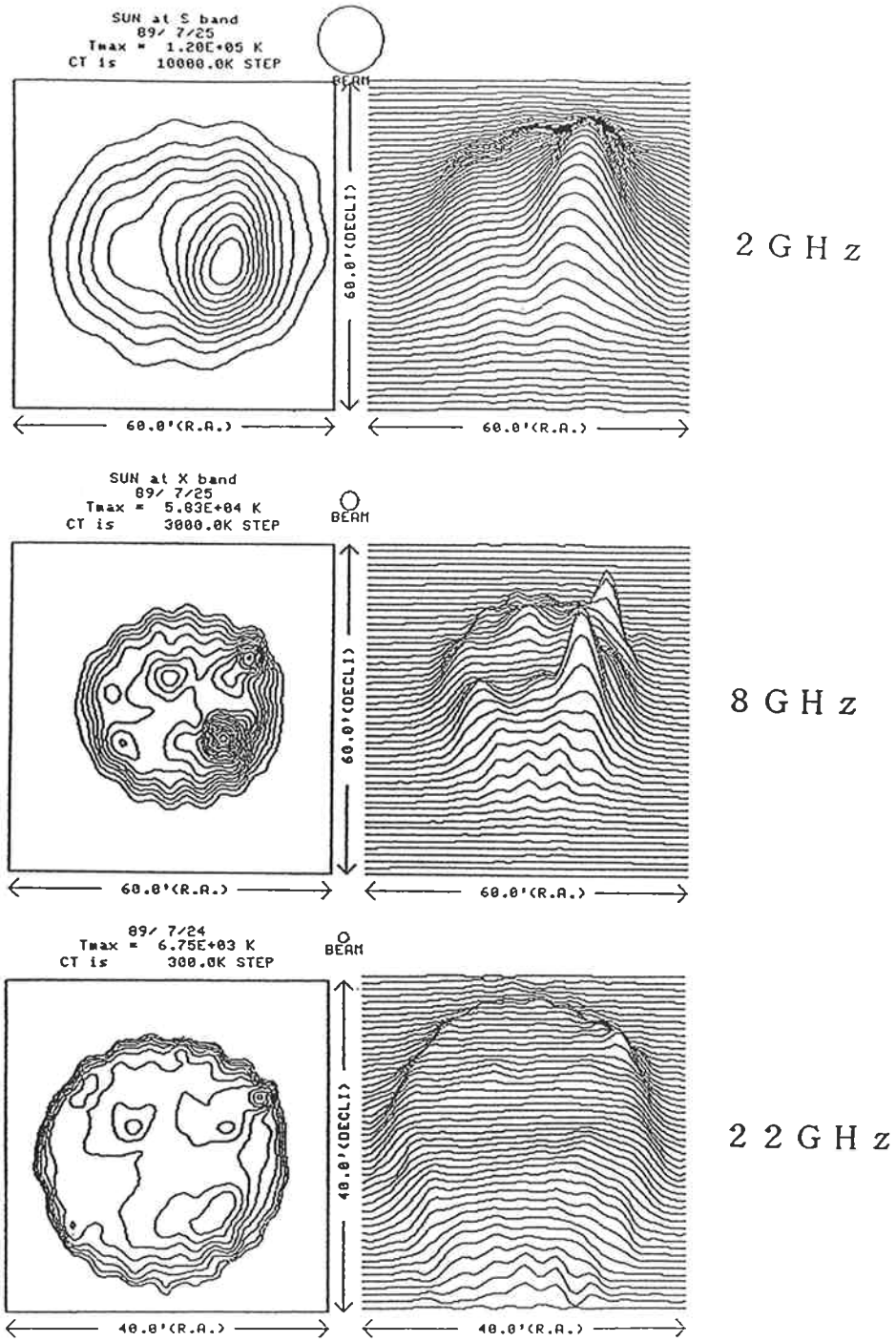

Fig. 14 Solar radio intensity maps at 2 GHz, 8 GHz, and 22 GHz.

Fig. 15 An acousto-optical spectrometer (AOS) developed at NRO. An optical diode-laser is used. The frequency resolution and the band width are 40 kHz and 40 MHz, respectively.

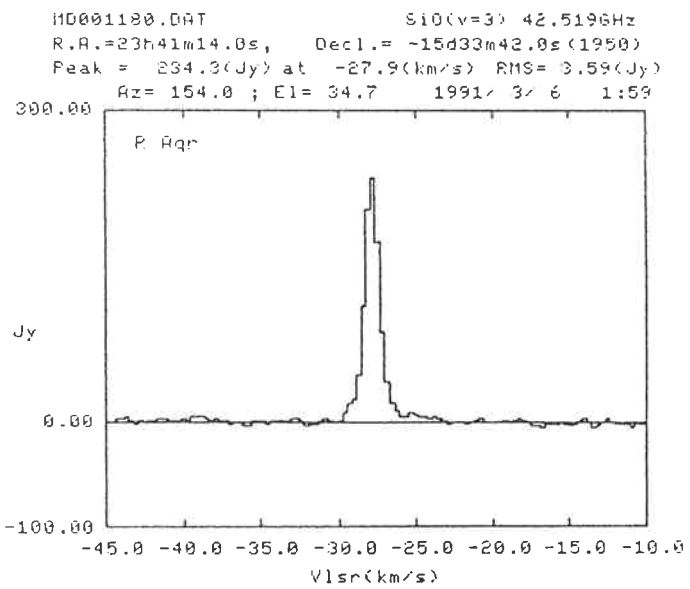

Fig. 16 SiO ($J = 1 - 0$, $v = 3$) maser spectra at 43 GHz. Integration time was 15 minutes and an AOS was used.